

Martian Core Analysis

Introduction

The study of a planet's interior is fundamental to understanding its **geological history, thermal evolution, and potential for past or present life**. For Mars, one of our closest neighbors, this is particularly important as it holds secrets about how the planet evolved, why it lost its magnetic field, and whether it could have once supported life. Mars has been the focus of numerous space missions, and with the recent **InSight mission**, we've gained groundbreaking data on Mars' interior, especially its crust, mantle, and core. This seismic data allows us to peer deep into the Martian planet, providing insights that were once only speculative.

The Martian core, in particular, has been a point of intrigue for planetary scientists. Unlike Earth, whose core is largely solid and liquid, Mars is thought to have a core that could either be fully or partially liquid. Understanding whether Mars' core is liquid or solid is key to answering some of the most pressing questions in planetary science, such as:

- Why does Mars have a weak magnetic field?
- How did its geological features form?
- And what implications does this have for future human exploration or even settlement?

One of the most powerful tools for understanding the internal structure of planets is **seismic waves**. These waves travel through the interior and interact with different layers of a planet, providing indirect but highly valuable information about its **composition, state, and structure**. In the case of Mars, seismic wave data from the InSight lander has allowed scientists to detect the presence of seismic waves traveling through Mars' interior. This data, particularly from P-waves (primary waves) and S-waves (secondary waves), can help us determine if the Martian core is liquid or solid.

Through a detailed analysis of how seismic waves propagate through the planet, including **shadow zones created by S-waves**, the reduction in velocity of P-waves, and other seismic signatures, we can make inferences about the state of the Martian core. This report delves into the core's characteristics by evaluating wave velocities, identifying key seismic patterns, and comparing findings with both theoretical models and observational data.

Objective

The goal of this analysis is not just to understand the Martian core but to use seismic wave data in a way that helps us make informed conclusions about its state, size, and composition. Specifically, we aim to determine whether the Martian core is liquid or solid by analyzing key seismic wave phenomena. The analysis involves several interrelated tasks, including the **detection of S-wave shadow zones, P-wave velocity reduction, and core radius calculations**.

1. **Seismic Waves and Their Role:** Seismic waves are the key to this analysis. After a seismic event, these waves travel through the planet's interior and interact with various layers. By analyzing how these waves behave, we can infer critical properties of the layers they travel

through. **P-waves**, which can pass through both solids and liquids, and **S-waves**, which can only travel through solids, provide complementary data. If S-waves are absent on the far side of Mars after a seismic event, this would indicate the presence of a liquid layer, as S-waves cannot travel through liquids. Similarly, any reduction in the velocity of P-waves when they pass through the core would signal a transition from solid to liquid, which would further support the liquid core hypothesis.

2. **Key Objectives:** This analysis seeks to answer some fundamental questions:

- (a) What are the velocities of P-waves and S-waves in Mars' mantle and core, and how do they differ?
- (b) Is there any evidence of an S-wave shadow zone on Mars, and what does this tell us about the core's state?
- (c) What is the core radius, and does this match with the seismic data obtained from the InSight mission?
- (d) How do the seismic observations of P-wave refraction support the hypothesis of a liquid core?

3. **Theoretical Calculations and Observations:** The core's state can be inferred by studying how seismic waves behave at the core-mantle boundary. Using **Snell's Law**, we will analyze how seismic waves refract when transitioning from the mantle to the core. Additionally, by comparing these theoretical calculations with actual seismic data from InSight, we aim to validate our understanding of the Martian core's state. This will include deriving the **P-wave and S-wave velocities** using known material properties like shear modulus and density.

4. **Verification and Refinement:** With the seismic data collected from Mars, we can also refine our calculations by comparing the estimated **core radius** with the seismic results. This will help in verifying whether the calculated values align with real-world data, and it will provide an opportunity to identify any discrepancies. These inconsistencies could be due to factors such as assumptions of uniform density or a simplified core model, which may not fully reflect the complexities of Mars' interior.

5. **Impact of Findings:** The ultimate aim of this research is not only to confirm whether Mars' core is liquid or solid but also to understand the broader implications of the core's state for Mars' geological evolution. A liquid core could explain Mars' lack of a global magnetic field and provide insights into its thermal history and the potential for past volcanic activity. This understanding is crucial for future missions to Mars, whether they involve scientific exploration or human settlement.

Module 1: Understanding Seismic Wave Velocities

Part 1

Seismic waves are vibrations in the earth that transmit energy and occur during seismic activity such as earthquakes, volcanic eruptions, and even man-made explosions. Majorly, there are two types of seismic waves, primary waves (P-waves) and secondary waves (S-waves). They are classified as body waves because they travel through the interior of planetary bodies.

1. Properties of P-waves:

- Also known as pressure waves
- These are the first waves to be recorded in the seismograph at the time of an earthquake

- Fastest seismic waves (about 1.7 times faster than S-waves)
- These are compression waves
- Travel through **solids, liquids, and gases**
- Compress and expand the material in the direction of wave propagation (longitudinal)

2. Properties of S-waves:

- Also known as shear waves
- These are the second waves to hit the seismograph
- Slower than P-waves
- Travel only through **solids**
- Cause the material to move perpendicular to the wave's direction (transverse)

Key Differences Between P-Waves and S-Waves:

Feature	P-Waves	S-Waves
Speed	Faster	Slower
Arrival	First to arrive	Second to arrive
Motion	Longitudinal (compressional)	Transverse (shear)
Medium	Solids, liquids, and gases	Solids only
Energy Transfer	Parallel to wave direction	Perpendicular to wave direction

Table 1: Key differences between P-waves and S-waves.

Part 2

The formulae for calculating the velocities of P-wave and S-wave are

$$V_p = \left(\frac{K + \frac{4G}{3}}{\rho} \right)^{\frac{1}{2}}$$

$$V_s = \left(\frac{G}{\rho} \right)^{\frac{1}{2}}$$

where,

$$K \text{ (bulk modulus)} = 25 \times 10^{10}$$

$$G \text{ (shear modulus)} = 1.0 \times 10^{10}$$

$$\rho \text{ (density)} = 3000 \text{ kg/m}^3$$

Plugging in the given values in the above formulae gives us

$$V_p = \left(\frac{25 \times 10^{10} + \frac{4 \times 1.0 \times 10^{10}}{3}}{3000} \right)^{\frac{1}{2}}$$

$$= \left(\frac{25 \times 10^{10} + 1.33 \times 10^{10}}{3000} \right)^{\frac{1}{2}}$$

$$= \left(\frac{26.33 \times 10^{10}}{3000} \right)^{\frac{1}{2}}$$

$$\boxed{V_p = 3574.60 \text{ m/s}}$$

and,

$$V_s = \left(\frac{1.0 \times 10^{10}}{3000} \right)^{\frac{1}{2}}$$

$$\boxed{V_s = 1825.74 \text{ m/s}}$$

Part 3

Given wave equation:

$$\rho \frac{\partial^2 U_i}{\partial t^2} = \frac{\partial \sigma_{ij}}{\partial x_j}$$

From Hooke's law, we have:

$$\begin{aligned} \sigma_{ij} &= \lambda \delta_{ij} (\nabla \cdot U) + \mu \left(\frac{\partial U_i}{\partial x_j} + \frac{\partial U_j}{\partial x_i} \right) \\ \frac{\partial}{\partial x_j} \sigma_{ij} &= (\nabla \cdot \sigma)_i = \nabla_j \cdot \sigma_{ij} \\ \Rightarrow \frac{\partial \sigma_{ij}}{\partial x_j} &= \nabla_j \left[\lambda \delta_{ij} (\nabla \cdot U) + \mu \left(\frac{\partial U_i}{\partial x_j} + \frac{\partial U_j}{\partial x_i} \right) \right] \\ &= \lambda [\nabla_j \cdot \delta_{ij} (\nabla \cdot U)] + \mu \nabla_j \left(\frac{\partial U_i}{\partial x_j} + \frac{\partial U_j}{\partial x_i} \right) \quad \text{where } \delta_{ij} = \begin{cases} 1, & i = j \\ 0, & i \neq j \end{cases} \\ &= \lambda \left[\frac{\partial}{\partial x_i} (\nabla \cdot U) \right] + \mu \frac{\partial}{\partial x_j} \left(\frac{\partial U_i}{\partial x_j} + \frac{\partial U_j}{\partial x_i} \right) \\ &= \lambda \left[\frac{\partial}{\partial x_i} (\nabla \cdot U) \right] + \mu \left(\frac{\partial^2 U_i}{\partial x_j^2} + \frac{\partial^2 U_j}{\partial x_i \partial x_j} \right) \\ &= \lambda \left[\frac{\partial}{\partial x_i} (\nabla \cdot U) \right] + \mu \left(\nabla^2 U_i + \frac{\partial \cdot (\nabla \cdot U)}{\partial x_i} \right) \\ \Rightarrow \boxed{\frac{\partial \sigma_{ij}}{\partial x_j} = \rho \frac{\partial^2 U_i}{\partial t^2} = (\lambda + \mu) \frac{\partial}{\partial x_i} (\nabla \cdot U) + \mu \nabla^2 U_i} \end{aligned}$$

where:

- σ_{ij} : Cauchy stress tensor
- u_i : Displacement vector
- λ : First Lamé parameter
- μ : Shear modulus (second Lamé parameter)
- x_i : Spatial coordinates

For P-wave and S-wave equations:

Displacement field has two components:

- Longitudinal component: Scalar potential ϕ
- Transverse component: Vector potential \mathbf{A}

$$\mathbf{U} = \nabla \phi + \nabla \times \mathbf{A}$$

- $\nabla \phi$ represents P-waves
- $\nabla \times \mathbf{A}$ represents S-waves

$$\nabla \cdot \mathbf{U} = \nabla^2 \phi + \nabla \cdot (\nabla \times \mathbf{A}) = \nabla^2 \phi \quad \Rightarrow \quad \nabla \cdot \mathbf{U} \text{ is determined by } \phi \text{ (P waves)}$$

$$\nabla \times \mathbf{U} = \nabla \times \nabla \phi + \nabla \times (\nabla \times \mathbf{A}) \quad \Rightarrow \quad \text{Shear waves are described by } \mathbf{A}$$

We have,

$$\rho \frac{\partial^2 U}{\partial t^2} = \mu \nabla^2 U + (\lambda + \mu) \nabla (\nabla \cdot U)$$

$$U = \nabla \phi + \nabla \times \mathbf{A}$$

$$\rho \frac{\partial^2}{\partial t^2} (\nabla \phi + \nabla \times \mathbf{A}) = \mu \nabla^2 (\nabla \phi + \nabla \times \mathbf{A}) + (\lambda + \mu) \nabla (\nabla \cdot U)$$

For P-wave equation, take ∇ on both sides $(\nabla \cdot U = \nabla^2 \phi)$

$$\rho \frac{\partial^2}{\partial t^2} (\nabla^2 \phi) = \mu \nabla^4 \phi + (\lambda + \mu) \nabla^2 (\nabla^2 \phi)$$

$$\rho \frac{\partial^2}{\partial t^2} (\nabla^2 \phi) = (\lambda + 2\mu) \nabla^4 \phi$$

$$\Rightarrow \boxed{\frac{\partial^2 \phi}{\partial t^2} = \left(\frac{\lambda + 2\mu}{\rho} \right) \nabla^2 \phi}$$

Wave equation for P-wave

$$\Rightarrow v_p = \sqrt{\frac{\lambda + 2\mu}{\rho}}$$

For S-wave equation, we have $\nabla \cdot U = 0 \quad \Rightarrow \quad \nabla^2 \phi = 0$

$$\rho \frac{\partial^2 U}{\partial t^2} = \mu \nabla^2 U + (\lambda + \mu) \nabla (\nabla \cdot U)$$

Take curl on both sides,

$$\nabla \times \left(\rho \frac{\partial^2 U}{\partial t^2} \right) = \nabla \times (\mu \nabla^2 U + (\lambda + \mu) \nabla (\nabla \cdot U))$$

$$\rho \frac{\partial^2}{\partial t^2} (\nabla \times U) = \nabla \times (\mu \nabla^2 U) + \nabla \times ((\lambda + \mu) \nabla (\nabla \cdot U))$$

$$\rho \frac{\partial^2 (\nabla \times U)}{\partial t^2} = \mu \nabla^2 (\nabla \times U)$$

$$\nabla \times U = \nabla \times (\nabla \times \mathbf{A})$$

$$\rho \frac{\partial^2}{\partial t^2} [\nabla \times (\nabla \times \mathbf{A})] = \mu \nabla^2 [\nabla \times (\nabla \times \mathbf{A})]$$

$$\Rightarrow \rho \frac{\partial^2}{\partial t^2} (\nabla \times \mathbf{A}) = \mu \nabla^2 (\nabla \times \mathbf{A})$$

$$\boxed{\frac{\partial^2}{\partial t^2} (\nabla \times \mathbf{A}) = \left(\frac{\mu}{\rho} \right) \nabla^2 (\nabla \times \mathbf{A})}$$

Wave equation for S-wave

$$\Rightarrow v_s = \sqrt{\frac{\mu}{\rho}}$$

Research Insights

1. Seismic Wave Velocities and Mars' Mantle:

- (a) A study of seismic wave propagation from **MIT Course Material** explains the fundamental equations governing P-wave and S-wave velocities in Earth's interior. Using the **stress** and **strain** tensor equations, **Hooke's Law** and the **Helmholtz equation**, the derivation of wave motion in an elastic and homogeneous medium is presented. The analysis shows that seismic wave behavior is influenced by Lamé parameters.
-

Module 2: Identifying Shadow Zones

- The **S-wave shadow zone** refers to the region on a planet's surface where **S-waves (secondary or shear waves)** are not detected. This is because when S-waves hit the liquid outer core, they get **absorbed or completely stopped** because liquids can't handle the **transverse wave motion**, which is why the existence of an S-wave shadow zone indicates the presence of a liquid core.
- If **S-waves (secondary waves)** are not detected on the opposite side of a planet from a seismic event, it suggests that the planet's core is in a **liquid state**. Here's why: S-waves cannot propagate through liquids because liquids do not have the **shear strength** to support the side-to-side (transverse) motion of these waves. If the core is liquid, the S-waves are absorbed or stopped entirely when they encounter the liquid core. This creates an **S-wave shadow zone** on the opposite side of the planet, where no S-waves are detected. The absence of S-waves on the far side is strong evidence for a liquid outer core.

Research Insights

1. Absence of S-Waves and Liquid Core:

- (a) In a study by **Lognonné et al. (2021)**, the **absence of S-waves** on the opposite side of Mars from a seismic event strongly suggested that the **Martian core is liquid**. This is similar to the Earth's outer core, where the lack of S-waves indicates a liquid state.
- (b) According to **Banerdt et al. (2020)**, data from the **InSight seismometer** detected **S-wave shadow zones** on Mars, which revealed a **liquid outer core**, confirming earlier theories about Mars' internal composition.

2. Comparison with Earth's S-Wave Shadow Zones:

- (a) A study published in **Nature Geoscience** compared the **S-wave shadow zones** of Mars with those on Earth and found striking similarities in their structure. This comparison reinforced the idea that Mars' outer core is molten, just like Earth's outer core.
- (b) Earth-like behavior was observed in the **InSight mission's seismic recordings** when **S-waves** were blocked by the core, demonstrating the fluidic nature of Mars' interior.

3. Seismic Data from InSight:

- (a) According to **InSight mission data (2021)**, the **S-wave shadow zone on Mars** extends from 105° to 180° from the seismic source, much like Earth's, reinforcing the presence of a **liquid outer core**. These results were consistent with previous models of planetary interiors.

4. S-Wave Diffraction and Core Structure:

- (a) **S-wave diffraction** at the **core-mantle boundary (CMB)** observed by the **InSight mission** suggests that the boundary between Mars' mantle and core is not just a simple liquid-surface transition but may involve complex variations in composition, which could influence seismic wave propagation.
-

Module 3: Calculating the Core-Mantle Boundary (CMB)

P-waves (primary waves) are compressional waves capable of traveling through both solid and liquid materials, but their velocities vary depending on the medium.

- The velocity of P-waves in the core is less than their velocity in the mantle.
- According to Snell's Law, a wave refracts away from the normal if there is an increase in the velocity and towards the normal if there is a decrease in the velocity.
- Hence, while travelling from mantle to core, P-waves refract towards the normal and while travelling from core to the mantle, they refract away from the normal.

The Analysis of InSight's seismic data revealed that P-waves traveling through Mars' core exhibit a decrease in velocity compared to their propagation in the mantle. This deceleration is indicative of a transition from a solid to a liquid medium.

Snell's Law of Refraction

The propagation of P-waves across the boundary follows Snell's Law:

$$\frac{\sin i}{v_1} = \frac{\sin r}{v_2}$$

Where:

- i : Angle of incidence (in the mantle).
- r : Angle of refraction (in the outer core).
- v_1 : Velocity of P-waves in the mantle.
- v_2 : Velocity of P-waves in the outer core (slower than in the mantle).

Because $v_2 < v_1$, the P-waves bend away from the normal as they enter the outer core.

Calculation

Here,

$$i = 30^\circ,$$

$$v_1 = 10 \text{ km/s},$$

$$v_2 = 8 \text{ km/s}$$

Using Snell's Law,

$$\frac{\sin 30}{10} = \frac{\sin r}{8}$$
$$r = \sin^{-1}\left(\frac{8 * \sin 30}{10}\right)$$

$$\boxed{r = 23.58^\circ}$$

Research Insights

1. Seismic Wave Refraction at the CMB:

- (a) **Snell's Law** predicts that when seismic waves pass from one medium to another with differing velocities, they bend or refract. For Mars, **P-waves** travel faster in the solid mantle than in the liquid core, creating a refracted P-wave angle that scientists can measure.
 - (b) In a study from **PNAS (2022)**, **InSight mission data** was used to calculate the **refraction angles** of P-waves at the core-mantle boundary. These results helped estimate the thickness of the Martian core and provided further evidence for a liquid outer core and provides a direct way of estimating the **core's size and composition**.
 - (c) The seismic behavior of **P-waves** at Mars' CMB was compared to Earth's CMB and yielded similar patterns of refraction, reinforcing the similarity between the Martian and Earth's core behavior.
-

Module 4: Determining Core Radius:

Given,

Total radius of Mars (R) = 3390 km

The depth to the core-mantle boundary (d) = 560 km

The core radius (R_c) = $R - d = 3390 \text{ km} - 560 \text{ km} = 2830 \text{ km}$

Hence, **Core Radius (R_c): 2830 km**

Verification with Seismic Data

- The InSight mission of NASA gathered a lot of new information about Mars' crust, mantle and core. According to this report, Mars' core is molten and considerably larger than expected, about **1,120 miles** (about 1,800 kilometers) in radius.
- Hence, the calculated core radius of 2830 km is **inconsistent** with the seismic data observations.

Possible Reasons for Discrepancy

- This discrepancy suggests that the **simple formula** used in the calculation might not be accurate enough for determining the core radius of Mars.

Research Insights

1. Seismic Radius Estimates:

- (a) Recent research from **PNAS (2022)** suggests that the Martian core's radius is approximately **1,780 to 1,810 km**, which is much smaller than earlier estimates of **2,830 km**. These refined estimates come from analyzing core-reflected seismic waves (ScS) observed by the **InSight seismometer**.

2. Cfrom Seismic Data:

- (a) The **InSight mission** has helped refine the core radius by detecting **reflections of seismic waves** from the core-mantle boundary. These reflections give a more accurate estimate of the core's size.

3. Core Composition

- (a) A paper by **Dehant et al. (2022)** discusses how **core size estimates** help infer the **core's composition**, indicating that the Martian core is likely a mixture of iron and lighter elements like **sulfur, carbon, and oxygen**. These elements contribute to the core's lower density and smaller radius.
-

Module 5: Verifying Core State:

Conclusion: Liquid Core

Based on the provided calculations, observations, and seismic wave behavior, the Martian core is likely liquid. Here's the reasoning:

Evidence from the Absence of S-Waves

S-Wave Behavior:

- S-waves (Secondary waves) cannot propagate through liquids because they rely on the shear strength of the medium.
- If S-waves are absent on the opposite side of Mars from a seismic event, it strongly indicates that the Martian core is liquid, as it cannot transmit shear waves.

Shadow Zones:

- The detection of S-wave shadow zone implies a boundary where the material transitions from solid to liquid (likely the core-mantle boundary).

Reduction in P-Wave Velocity

P-Wave Refraction:

- P-waves (Primary waves) can travel through both solids and liquids but move slower in liquids due to the lack of shear modulus.
- A significant reduction in P-wave velocity when entering the Martian core suggests that the core has liquid properties.

Comparison with Earth's Core:

- On Earth, P-waves slow down at the liquid outer core. A similar behavior in Martian seismic data supports the hypothesis of a liquid core.

Justification of a Liquid Core

- The absence of S-waves in the core region eliminates the possibility of a fully solid core.
- The observed reduction in P-wave velocity within the core aligns with the properties of a liquid medium.

Conclusion: These seismic characteristics indicate that the Martian core is not solid but instead liquid or at least contains a significant liquid layer.

Research Insights

1. Observations of Core-Diffracted Seismic Waves:

- (a) A recent study by **Knapmeyer et al. (2023)** explored **core-diffracted seismic waves**, which occur when seismic waves travel through the core and are reflected or refracted back to the surface. This study, based on **InSight mission data**, suggested that the Martian core is likely liquid due to the observed **diffracted waves**, which occur due to the core's **liquid outer layer**. These waves provided further evidence for a liquid outer core based on their distinct travel patterns.
- (b) In their study published in **Geophysical Research Letters**, the researchers observed that the core-reflected waves from the Martian mantle were **distinctly diffracted**, which helped in pinpointing the **liquid nature** of the core

2. Thermal and Density Profile of Mars' Core:

- (a) **Rivoldini et al. (2023)** conducted a study that linked the **core's thermal profile** to the seismic data. They found that if Mars had a **solid core**, the **heat flow** from the interior would be insufficient to maintain the liquid state of the outer core. This study suggested that the **thermal gradient** observed in the Martian mantle indicates the presence of a **liquid outer core**. Their **thermal model** predicted that the core must be at a temperature high enough to remain molten, which aligns with the seismic data showing slow P-wave velocities and absence of S-waves.
- (b) The **density variations** observed in seismic data from the **InSight mission** also confirmed the **lighter elements** present in the core (such as sulphur and carbon), which likely contribute to the lower density compared to pure iron. This also reinforces the idea that the Martian core is likely liquid, as these elements would lower the melting point, allowing the core to remain molten.

3. Mars' Core Composition from Seismic Data:

- (a) In a study published by **Fischer et al. (2022)** in **Nature Geoscience**, the authors used **seismic velocity inversions** to infer the **composition** of Mars' core. The data revealed that the **outer core is likely composed of a mixture of iron, nickel, sulphur, and oxygen**, elements that are typically found in **liquid cores**. The study used **P-wave** and **S-wave** velocity models to infer the presence of a molten outer core, and suggested that the **core's composition** differs from Earth's, likely due to **Mars' lower planetary mass** and cooler temperature.
- (b) This research used **Seismic Inversion Models** to match the observed P-wave velocity reductions with core compositions that are not purely iron, showing that Mars' liquid core contains significant amounts of lighter elements, which support the theory of a molten core.

4. Evidence from the InSight Seismic Array:

- (a) The **Seismic Array Study** of Mars, particularly focused on the **core-mantle boundary (CMB)**, shows clear evidence of **P-wave refraction** at the boundary between the mantle and core. A study in **Journal of Geophysical Research (2022)** analyzed **seismic data from InSight** and found that the **P-wave velocity decreases significantly** when passing through the core, providing additional evidence that Mars has a **liquid outer core**.
- (b) The seismic array data collected from **InSight** also confirmed the presence of **strong core reflections** from the core-mantle boundary, which further supports the liquid state hypothesis. These **reflections** were found to correspond to liquid-core behavior seen in other planetary bodies.

5. Mars' Magnetic Field and Liquid Core Evidence:

- (a) Another piece of evidence linking Mars' liquid core to its **lack of a magnetic field** comes from **Mound et al. (2022)**. This study indicated that Mars' lack of an active magnetic field, unlike Earth's, is likely due to a **non-convective liquid outer core**. If the core

were solid, it could potentially generate a magnetic field through convection. However, due to the liquid nature of Mars' outer core, this dynamo effect does not occur. The absence of magnetic field activity suggests that, although Mars' core is liquid, it is not undergoing **active convection**, which would otherwise generate a magnetic field. This aligns with the observations from seismic data, indicating that the **core's liquid outer layer** has cooled and is no longer convecting as effectively as Earth's outer core.

6. Implications for Mars' Geological Evolution:

- (a) **Gagnepain-Beyneix et al. (2022)** further explored the **geological implications** of a liquid core, suggesting that Mars' **tectonic activity** and volcanic history might have been driven by the presence of a molten outer core. This could have influenced the planet's early geological activity, including the formation of large volcanoes like **Olympus Mons** and **Tharsis**. A liquid core may have played a key role in the early thermal history of the planet, sustaining volcanic activity and crust formation during Mars' younger years.
- (b) The **lack of core convection** in the current day is also consistent with Mars' **low levels of tectonic activity**, as the planet has cooled and the core's convective processes have largely ceased. This shift has implications for understanding the planet's **thermal evolution**, which has slowed, contributing to the current **lack of significant seismic activity**.

7. Comparative Analysis of Mars and Other Planets:

- (a) A comparative study by **Dohm et al. (2021)** compared Mars' seismic data with that of other planets like Venus and Mercury. The study suggested that while **Venus also has a molten core**, its **core dynamics** may be different due to its **higher thermal energy**, which could explain its current volcanic activity. Mars, on the other hand, has **lower thermal gradients in its core**, resulting in a less active core with no current volcanic activity.
- (b) **Mercury** also exhibits a partially liquid core, but due to its smaller size, the cooling rate is much faster, leading to a **more solidified core**. This comparison with **Venus and Mercury** helps to refine our understanding of Mars' unique internal structure, which may have experienced a **cooling process** more similar to Mercury's over geological time scales.
- (c) Core and size and Magnetic Field
 - i. Mars lacks a magnetic field because its core is inactive, unlike Earth's which has a convecting liquid core generating a magnetic field.
 - ii. Venus shows weak magnetic anomalies, suggesting a partially convecting core, whereas Mars has no such anomaly.
 - iii. Smaller planets like Mercury cool faster, leading to a solidified core, whereas Mars' larger size allowed its core to remain molten longer.

Module 6: Seismic Signal Processing Using ML

Extraction of Amplitude, Frequency, and Phase Shifts from Seismic Waveforms

1. Amplitude:

Extraction: The amplitude can be extracted by identifying the highest point (peak) of the waveform or using the signal's envelope. Peak-to-peak amplitude (difference between maximum and minimum points) provides additional insight into wave intensity and energy.

Significance: Amplitude is used to estimate energy, stress drop, and seismic wave magnitude.

2. Frequency:

Extraction: Frequency is derived using Fourier Transform (FFT), which converts the time-domain waveform into the frequency domain. The dominant frequency is the one with the highest amplitude in the frequency spectrum.

Significance: P-waves and S-waves often have different frequencies, which helps distinguish them. Frequency is also related to the wavelength and velocity of seismic waves, aiding in distance and core property estimations.

3. Phase Shift:

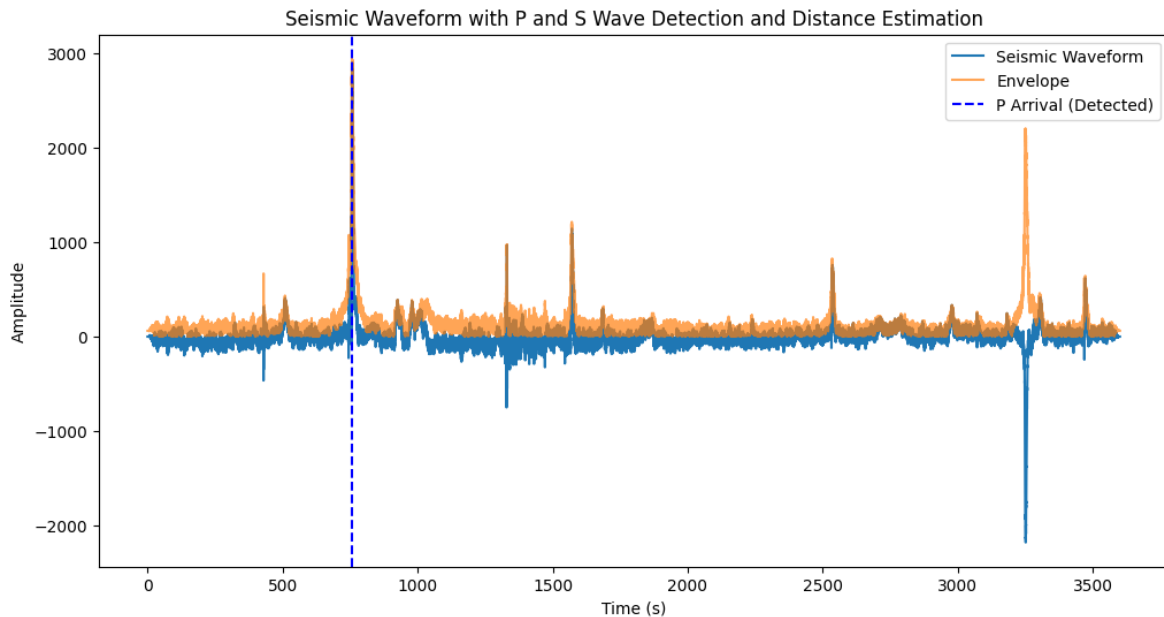
Extraction: Phase shifts can be identified by measuring time differences between wave arrivals (e.g., P-wave and S-wave). Changes in the medium (such as crossing the Earth's core) cause phase delays, which are detected by comparing these arrival times.

Significance: Phase shifts help identify shadow zones where S-waves disappear due to the liquid outer core, and they provide information about seismic wave propagation and the Earth's internal structure.

Approach

1. Analyzing Seismic Waveforms

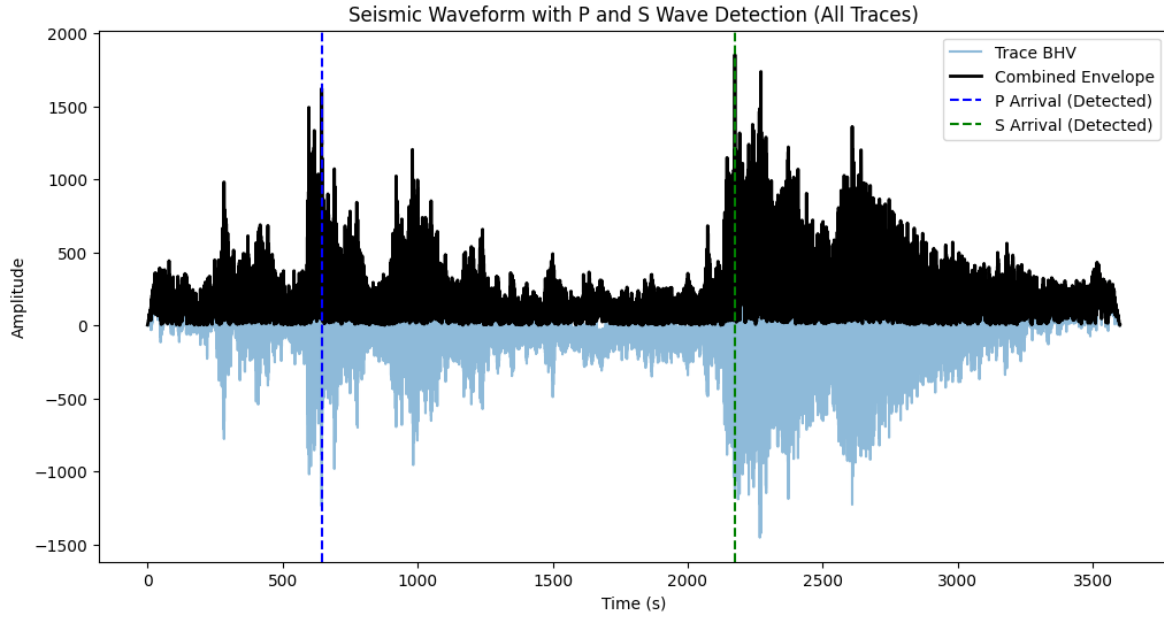
The process begins with analyzing seismic MiniSEED files, which contain waveform data. The goal is to identify key seismic wave events: P-waves and S-waves. P-waves, being the fastest, arrive first, while S-waves are slower and do not travel through liquid regions, creating shadow zones.



2. Extracting Key Features

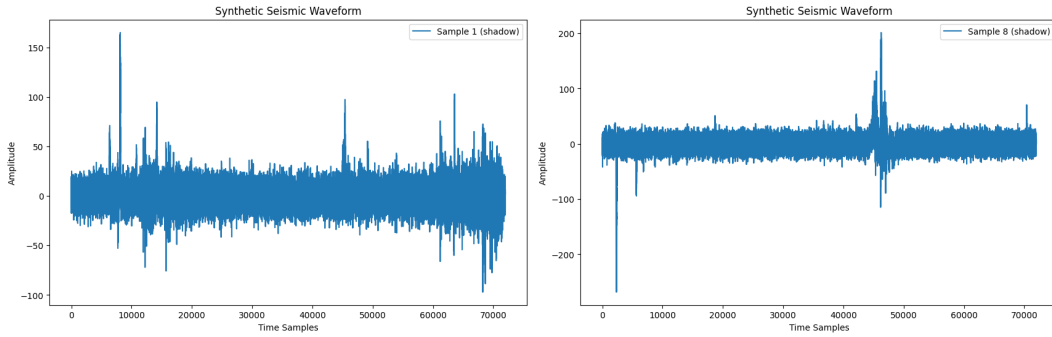
Several key features are extracted from the waveform data to aid in classification:

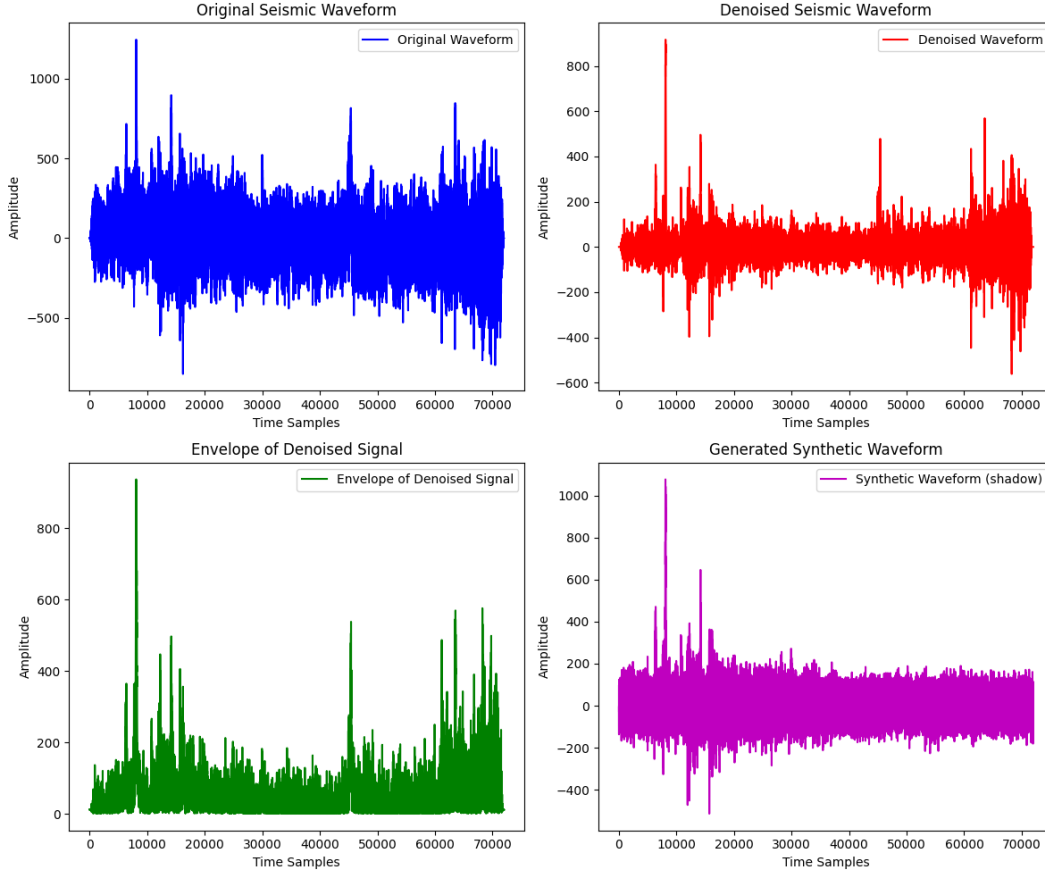
- Amplitude** is measured to determine the strength of the wave. It is derived using the signal's envelope, which highlights peaks and troughs.
- Frequency** is extracted through the Fourier Transform, which converts the signal into the frequency domain. The dominant frequency helps differentiate between wave types.
- Phase shifts** are detected by measuring the time difference between the arrival of P-waves and S-waves. This time gap provides critical information on the wave's travel path and any interruptions in propagation caused by core structures.



3. Generating Synthetic Data

To enhance the dataset, synthetic seismic waveforms are generated. These synthetic signals replicate real-world scenarios, including both shadow and non-shadow zones. Random shifts, distortions, and Gaussian noise are added to make the synthetic data more realistic. This helps increase the diversity of training samples for the machine learning models.





4. Building and Evaluating Machine Learning Models

Features from both real and synthetic data are used to train various supervised machine learning models. Models such as Random Forest, Gradient Boosting, SVM, and XGBoost are employed to classify seismic events into shadow and non-shadow zones. Feature importance is evaluated to understand which aspects of the waveform (e.g., amplitude, frequency, or wavelet features) most strongly influence the classification.

5. Model Optimization and Evaluation

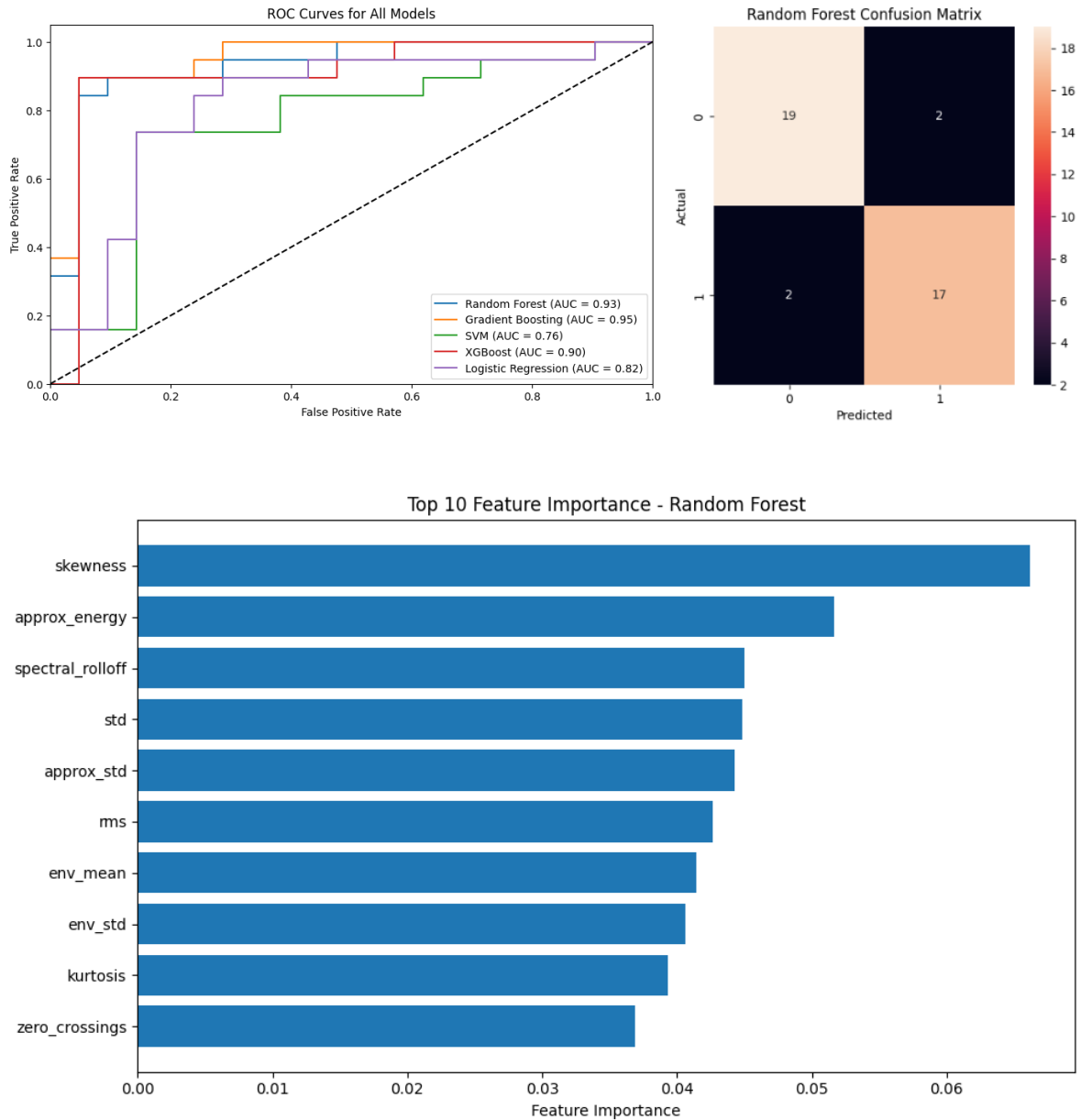
GridSearchCV is used for hyperparameter tuning to optimize each model's performance. The models are evaluated using metrics like accuracy, precision, recall, and F1 score. Visualization tools such as confusion matrices and ROC curves provide further insight into model's effectiveness.

6. Visualization of Results

The process concludes with plots that summarize key results:

- Confusion matrices display how well each model distinguishes between shadow and non-shadow zones.
- ROC curves illustrate the models' ability to discriminate between classes.
- Feature importance plots highlight the most influential features, offering interpretability for model predictions.

This approach integrates physics-based analysis and machine learning to effectively classify seismic data, aiding in the detection of planetary core properties.



Out of all the models used, Random Forest gave best results.

Module 7: Predicting Core Radius Using Regression

This module focuses on analyzing seismic and geological data from multiple .bm files to predict depth (or radius) within a planet's layers. Here's how the process unfolds:

The data comes from several **.bm** files, each containing details about the planet's internal layers. These files include key properties like:

- Radius (distance from the planet's core)
- Density (ρ)

- Wave velocities (vpv, vsv, vph, vsh)
- Elastic properties (qka, qmu, eta)

The region upto which S-wave velocity (vsv and vsh) is zero helps define the boundary between the solid mantle and the liquid outer core. For more details, the .bm files are sourced from [Pre-Mission InSights on the Interior of Mars](#)

We tried Random Forest and XGBoost, and XGBoost gave better results.

Module 8: Anomaly Detection in Seismic Data

Anomaly Type	How It Appears in a Waveform	Detection Method	Geological Feature on Mars
Spike	Sudden, sharp increase in amplitude	<ul style="list-style-type: none"> - High amplitude threshold detection - DBSCAN for outliers - Autoencoder detects high reconstruction error 	Marsquakes, impact events, stress release in crust
Dropout	Sudden signal loss (flatline or near-zero amplitude)	<ul style="list-style-type: none"> - Amplitude thresholding (near-zero values) - DBSCAN detects isolated points - Autoencoder flags unexpected signal loss 	Subsurface voids, porous rocks, potential liquid water reservoirs
Noise Burst	High-amplitude random noise over a short duration	<ul style="list-style-type: none"> - Spectral analysis (Fourier Transform) - Wavelet decomposition for transient signals - Autoencoder detects bursty patterns 	Geothermal activity, gas movement, meteorite impacts
Frequency Shift	Gradual change in dominant frequency over time	<ul style="list-style-type: none"> - Spectrogram analysis (STFT) - K-Means clustering for frequency shifts - Autoencoder detects waveform distortions 	Lithology changes, underground fractures, subsurface ice melting

Table 2: Seismic Anomalies on Mars & Their Geological Significance

This module focuses on identifying and classifying different types of anomalies in synthetic seismic waveforms. These anomalies include spikes, dropouts, noise bursts, and frequency shifts, which can disrupt normal seismic readings. The workflow can be broken down as follows:

1. Data Loading and Setup

Synthetic MiniSEED files are used to simulate seismic data. Along with these files, a CSV file provides labels that indicate where and what type of anomalies are present. This data is essential for training and evaluating the anomaly detection process.

2. Threshold Generation

The waveform data is analyzed in smaller windows (segments) to extract key features. Each window provides information like:

Feature	Description
Amplitude	Peaks in the waveform indicating sudden spikes.
Kurtosis	Measures the "sharpness" or "peakiness" of the signal, useful for detecting outliers.
Standard Deviation	Low values may suggest a dropout where the signal becomes flat or inactive.
Zero Crossings	Number of times the waveform crosses the baseline, indicating signal variations.
Energy	High energy levels may indicate a noise burst.
Dominant Frequency	Changes in frequency are analyzed to detect frequency shifts.

Table 3: Signal Analysis Features

3. Synthetic Data Generation with Anomalies

To enhance model performance, synthetic seismic waveforms are generated with predefined anomalies. This allows the model to learn how different anomalies manifest in the data. Various anomalies such as spikes, dropouts, noise bursts, and frequency shifts are introduced to simulate real-world scenarios. The **DBSCAN (Density-Based Spatial Clustering of Applications with Noise)** algorithm is applied to further identify clusters and anomalies within the features.

- **Eps (epsilon):** Defines the maximum distance between two points to be considered part of the same cluster.
- **Min Samples:** Specifies the minimum number of points required to form a dense region or cluster.

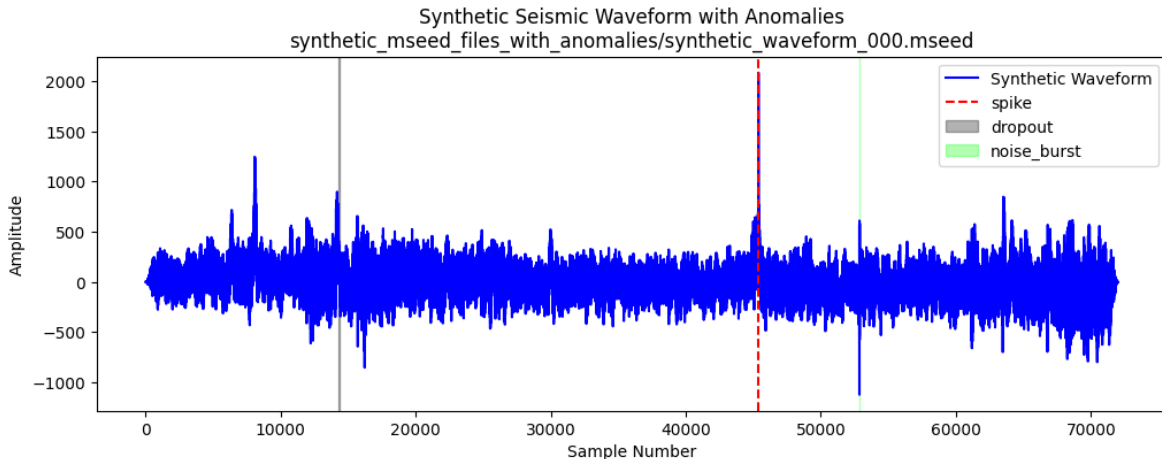
This clustering approach aids in separating normal points from outliers in the feature space.

4. Assigning Labels

The extracted features are matched with the labeled data to determine if an anomaly is present within each window. The labels specify the type of anomaly:

Term	Description
Spike	A sharp, sudden increase in amplitude.
Dropout	A period where the signal loses variation.
Noise Burst	A sudden, high-energy event.
Frequency Shift	A significant change in the waveform's dominant frequency.

Table 4: Signal Anomalies



5. Threshold Optimization

Once features and labels are ready, optimal thresholds are calculated for each anomaly type. This involves testing various threshold values to find the one that best separates normal and abnormal signals and using the F1 score to measure the balance between precision and recall, ensuring the detection method is both accurate and reliable.

6. Evaluation and Results

The module concludes by summarizing the optimal thresholds and performance scores for each anomaly type. The F1 scores provide insight into how well each detection method works.

Module 9: Training Physics Informed Neural Network for simulation of P & S wave velocities

Introduction

In this module we aim to build a **Physics-Informed Neural Network (PINN)** that predicts seismic wave velocities (P-wave and S-wave velocities) within the Martian interior. Seismic waves, including primary waves (P-waves) and secondary waves (S-waves), propagate through different layers of the planet and their velocities provide valuable insights into the planet's internal structure. The model developed here leverages both data-driven machine learning techniques and physical principles to predict these velocities. The training process integrates a neural network that respects the governing partial differential equations (PDEs) of seismic wave propagation.

Neural Network Architecture

The model uses a **feed-forward neural network** architecture with multiple layers to predict seismic velocities. The network is designed to learn from data and simultaneously satisfy the physics constraints derived from the governing equations of seismic wave propagation. Specifically, the model is trained with two sources of loss: **data-driven loss**, which measures the difference between predicted and actual seismic velocity data, and the **physics-driven loss**, which ensures that the predictions respect the underlying physical laws governing wave propagation.

The architecture employed in this model consists of several fully connected layers. The neural network's activation function was chosen as the **hyperbolic tangent (Tanh) function**, which is known for its smooth output and better handling of the physics-based problem compared to other activation functions such as **Swish**.

The model takes as input the normalized radius of Mars and outputs the predicted seismic velocities for both P-waves and S-waves in the Martian interior. The architecture is designed with layers ranging from **1 input neuron** (representing the radius) to **4 output neurons** (representing the velocities of the different seismic waves).

Physics-Informed Loss Function

A core component of the PINN is the incorporation of the wave equation residuals in the loss function. These residuals are derived from the governing physics of seismic wave propagation in a spherical planet. The physics loss ensures that the neural network predictions obey the PDEs that govern wave propagation.

For P-waves, the governing equation is:

$$\frac{d^2 v_{pv}}{dr^2} + \frac{2}{r} \frac{dv_{pv}}{dr} = 0$$

where v_{pv} is the P-wave velocity and r is the radial distance.

Similarly, for S-waves, the equation becomes:

$$\frac{d^2 v_{sv}}{dr^2} + \frac{2}{r} \frac{dv_{sv}}{dr} = 0$$

where v_{sv} is the S-wave velocity.

The neural network outputs predicted velocities for both P-waves (v_{pv}) and S-waves (v_{sv}), which are then used to compute the residuals of these wave equations. The first and second derivatives of the velocities with respect to the radial coordinate r are computed using **automatic differentiation**. These residuals are penalized in the loss function to ensure that the predicted velocities satisfy the wave propagation equations.

Data Preprocessing and Normalization

The input data consists of various seismic velocity profiles from Mars provided across different radial positions, which are extracted from the same **.bm** files that were used for Module-7. Before feeding the data into the neural network, the dataset is normalized to **zero mean** and **unit variance** for the velocity components. This normalization helps the network to train more efficiently and ensures that each feature contributes equally to the model’s performance.

Training Strategy and Optimization

The model is trained using the **AdamW optimizer**, which is an extension of the Adam optimizer that includes **weight decay** for **regularization**. The learning rate is initially set to 0.001, and a **learning rate scheduler (ReduceLROnPlateau)** is employed to adjust the learning rate during training based on the progress of the model. The physics-based residuals are combined with the data-driven loss to form the total loss. The final loss is a weighted sum of the two, where the weight on the physics loss is empirically set to 0.001. The optimizer is used to minimize this loss function during training, with gradient clipping applied to prevent gradient explosion, which is a common issue when training deep neural networks.

Evaluation and Results

After the model is trained, it is evaluated by comparing the predicted seismic velocities against the actual data. The comparison is visualized by plotting the actual versus predicted velocities for each of the seismic wave types (P-waves and S-waves) across different radial positions. The results are presented in a set of subplots, each depicting a specific velocity profile for the Martian interior. The trained model is expected to capture the general trends of the observed seismic data while also satisfying the physical laws governing wave propagation.

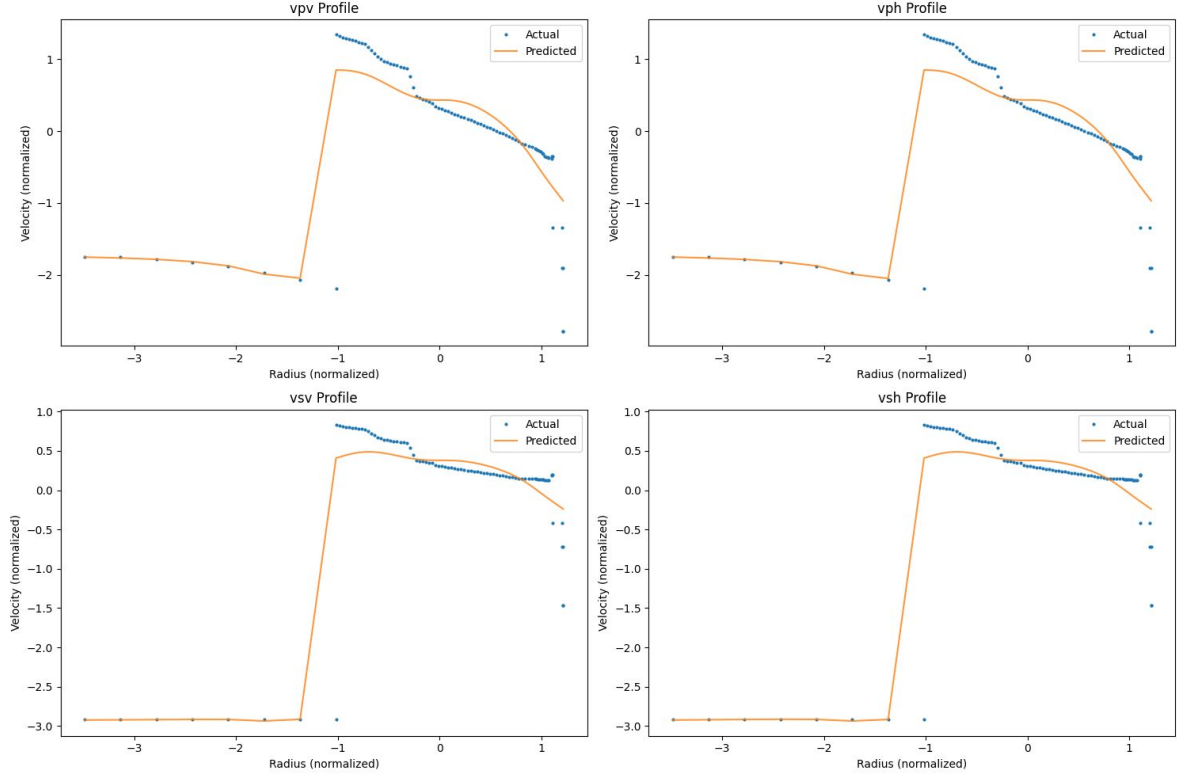


Figure 1: Comparison of Actual and Predicted Velocity Profiles for P-waves and S-waves Across the Martian Interior Radius

Challenges and Limitations

Despite the promising approach and results, several challenges and limitations were encountered during the development and implementation of the Physics-Informed Neural Network (PINN) for Mars seismic velocity prediction. These challenges include data-related issues, model limitations, computational complexity, and the inherent uncertainties in planetary seismic modeling.

1. Data Quality and Availability

One of the major limitations of this approach is the lack of high-quality, extensive, and well-annotated seismic data from Mars. While Earth-based seismic models and datasets are readily available for training and validation, Martian seismic data is sparse and often inferred indirectly from planetary missions. This limited data poses challenges for training a robust machine learning model. The lack of sufficient data can lead to overfitting or poor generalization, which compromises the predictive accuracy of the model.

Furthermore, data normalization, while effective in standardizing input features, can also mask the underlying physical variations within the dataset. This can cause the model to underperform when applied to new or unseen data, especially if the data distribution differs significantly from the training set.

2. Complexity of Physics-based Loss Function

The integration of physical principles into the loss function is a powerful tool for enforcing realistic predictions, but it also introduces a set of challenges. The computation of second-order derivatives for wave velocities requires high precision in gradient calculations, which can be computationally expensive and prone to numerical instability. Moreover, the nonlinearities introduced by the activation functions in the neural network might conflict with the smooth behavior expected from the physical wave equations, leading to challenges in convergence during training. Additionally, the balance between the data loss and physics loss in the total loss function is critical, and choosing the correct weight for the physics term (e.g., 0.001 in the current implementation) is nontrivial. A wrong weighting could lead to a model that overemphasizes data

fitting or physics constraints, reducing overall performance. Finding the optimal trade-off requires extensive experimentation and domain knowledge.

3. **Model Generalization and Overfitting** The neural network, although capable of approximating complex functions, may struggle to generalize when exposed to data that differs from the training set. The overfitting problem is especially pronounced when the dataset is small or highly specific, such as the Martian seismic data. In such cases, the model might memorize the training data instead of learning the underlying physical principles, leading to poor performance on new, unseen data.

Furthermore, as the model complexity increases (e.g., adding more layers or neurons), the risk of overfitting escalates. Regularization techniques like weight decay and gradient clipping help mitigate this issue, but they do not eliminate it entirely. A better understanding of how the model’s architecture interacts with the physics constraints is essential to improve generalization.

4. **Computational Cost and Training Time** Training a deep neural network with physical constraints is computationally expensive. The necessity of computing gradients for second-order derivatives of seismic velocities (i.e., the wave equations) adds significant computational overhead. In large datasets or with highly complex models, this can lead to prohibitive training times, especially when using high-precision gradient calculations.

Moreover, the use of automatic differentiation to compute second derivatives introduces additional complexity in the backward pass, which can significantly increase memory usage. This makes it challenging to train the model on a large scale, requiring powerful hardware resources or distributed computing, which may not always be available.

5. **Hyperparameter Tuning and Convergence Issues** The success of training a deep neural network largely depends on the careful selection of hyperparameters such as the learning rate, batch size, number of layers, and neurons per layer. The optimization process for the PINN involves both minimizing data-driven losses and physics-based residuals. Finding the right balance between these two sources of loss and tuning the optimizer’s parameters (e.g., learning rate schedule and weight decay) is a delicate task.

While the ReduceLROnPlateau scheduler helps in adjusting the learning rate, the model’s convergence can still be slow, especially when the physics loss and data loss are competing. The optimization landscape is complex due to the combination of physical constraints and the need for large-scale data fitting. This can lead to slow convergence or the model getting stuck in local minima.

6. **Incomplete Physics Model** The current model assumes a simplified form of the wave equations that may not fully capture all the complexities of Martian seismic wave propagation. For example, the model does not incorporate effects such as heterogeneous materials, anisotropy, or attenuation that might influence seismic velocities. These physical effects could lead to discrepancies between the predicted and actual velocities, especially if the Martian interior exhibits such complexities that are not captured by the simplified wave equations used in the model.

Moreover, the model assumes that the physical laws governing wave propagation are static and do not account for time-dependent or temperature-dependent variations that might occur within the Martian interior. Including these factors could improve the accuracy of predictions but would also complicate the model further.

7. **Lack of Interpretability** Although the PINN approach combines machine learning with physics, the interpretability of the model’s predictions remains limited. Understanding how the network learns the underlying physical principles or why it makes certain predictions is difficult due to the black-box nature of deep learning models. This lack of transparency can be problematic in scientific applications where interpretability and understanding of model behavior are crucial for trust and validation.

A deeper exploration into techniques that enhance the interpretability of the model, such as saliency maps or feature importance analysis, would be necessary for making the model’s decision-making process more transparent.

3D Visualization

A MATLAB code is written which visualizes the Martian interior and simulates the propagation of seismic waves (P-waves and S-waves) based on seismic parameters. It creates a 3D model of the Martian core, mantle, and crust, and uses spheres to represent each layer. A quarter of these spheres is cut to reveal the internal structure. The simulation animates the propagation of seismic waves from a randomly selected epicenter above the mantle. P-waves (green) propagate through all layers, while S-waves (red) stop at the mantle-core boundary. Lighting, textures, and wavefront properties enhance the visualization, and the animation updates the wavefronts at each time step. The code includes visual markers for the epicenter and legends to label the various components.

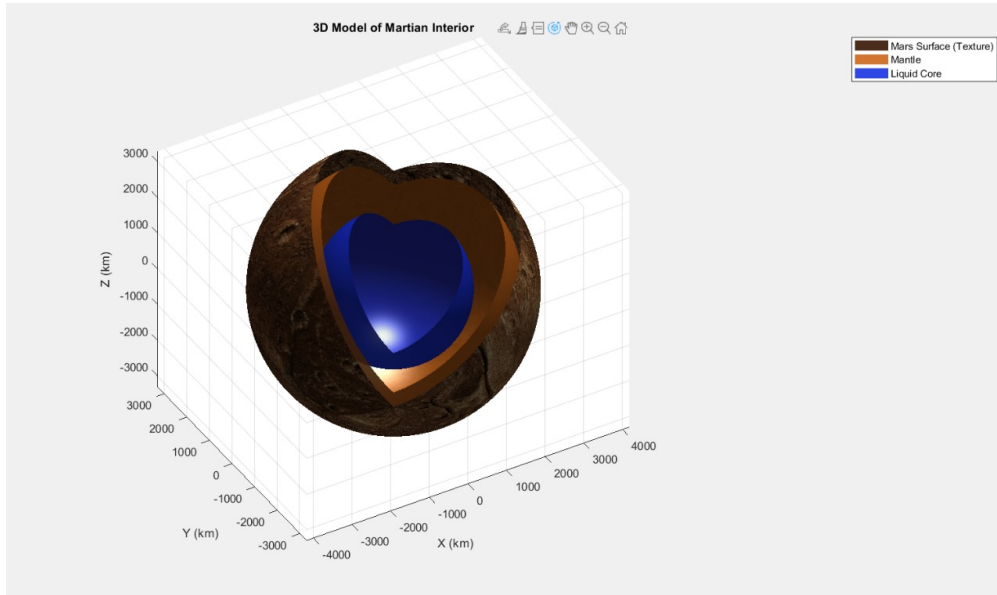


Figure 2: 3D Model of Martian Interior

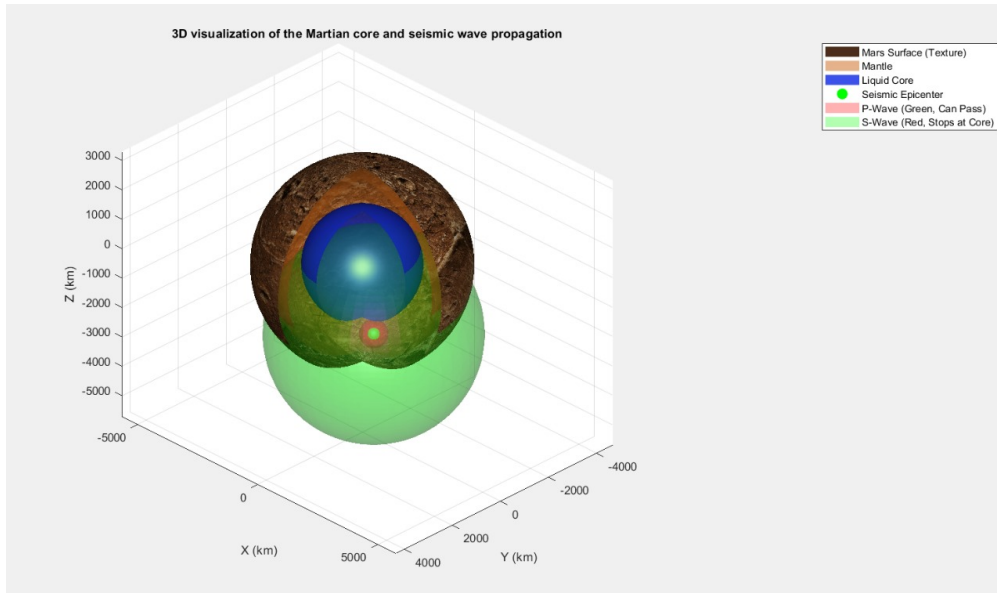


Figure 3: 3D Visualization of the Martian Core and Seismic Wave Propagation

Conclusion

This report explores the use of Physics-Informed Neural Networks (PINN) to predict seismic wave velocities in the Martian interior, combining data-driven and physics-based methods. By integrating synthetic data generation, machine learning models (e.g., Random Forest, XGBoost), and anomaly detection, the study successfully simulates seismic zones and predicts P-wave and S-wave velocities. Despite challenges like limited data, model generalization, and computational complexity, the approach offers valuable insights into Mars' internal structure and highlights the need for improved data quality, model optimization, and more complex physical models for future advancements in planetary seismic research.